# $^1$H n.m.r. relaxation studies and lineshape analysis of aqueous sodium carboxymethylcellulose

**Klaus Hofmann and Hyoe Hatakeyama***

*National Institute of Materials and Chemical Research, 1-1, Higashi, Tsukuba, Ibaraki 305, Japan*

*(Received 3 September 1993; revised 8 October 1993)*

The $T_1$ and $T_2$ proton n.m.r. relaxation times of water in aqueous sodium carboxymethylcellulose (NaCMC), with water contents below 2 $g_{H_2O}/g_{CMC}$, were measured between 340 and 120 K. The n.m.r. study revealed that (1) a distribution of correlation times and a correction of the Bloembergen, Purcell and Pound (BPP) theory for rigid lattice protons at low temperatures is necessary to simulate $T_2$ as a function of temperature, (2) non-freezing water is associated with two energetically distinct sorption sites, and (3) non-freezing water exhibits a temperature dependent motional anisotropy. Above 260 K, water at high-energy sites is responsible for an increase of $T_2$ with decreasing temperature. Below 260 K, $T_2$ shows a two-step decline that is caused by translational motion of the water molecules at the higher temperature and by rotational motion in the lower temperature region. The above mentioned motions are attributed to the motion of water molecules associated with lower-energy binding sites. At temperatures below 200 K, a Pake-type lineshape can be observed due to the increasing number of immobile water proton pairs. From a simulated lineshape analysis, the ratios of rotating to stationary water molecules were calculated as a function of temperature and water content.

**(Keywords: carboxymethylcellulose; n.m.r. relaxation; lineshape analysis)**

## INTRODUCTION

The study of water sorbed onto hydrophilic natural macromolecules, such as polysaccharides and polysaccharide electrolytes, has attracted interest for a long time[1-3]. A knowledge of the specific water–polymer interaction is essential for an understanding of the macroscopic properties of hydrated polymer materials. Macromolecular sorbed water is different from bulk water; depending on the moisture content, different types of water have been identified[4,5]. The nomenclature describing the various types of sorbed water is not well defined but a basic distinction can be made between *non-freezing* and *freezing* water. Non-freezing water does not show any first-order phase transition and remains as a viscous liquid below 0°C. It has also been associated with the term *bound* water[6,7], although the notion that all non-freezing water is strongly bound to the host molecule has been challenged[5,8]. Beyond a certain moisture content freezing water exists alongside non-freezing water. It forms ice upon cooling, but very often in a supercooled state. It is also known as *loosely bound* or *free* water. Thermal and nuclear magnetic properties of bound water, however, are different from those of free water[9]. Polyelectrolyte cellulosic systems also contain water associated with the counterion and it has been reported that the presence of counterions has an influence on the ratio of non-freezing to freezing water[10].

Due to the site-specific environments, it is assumed that various types of non-freezing waters could be distinguished from freezing water by their motional and energetic characteristics, such as correlation time and binding energy. Differential scanning calorimetry (d.s.c.) has been widely used to differentiate between freezing and non-freezing waters and to calculate their relative abundance[1,6,11]. However, thermal methods do not give information about the motional states of the sorbed water molecules. These phenomena can be studied efficiently by nuclear magnetic resonance (n.m.r.) spectroscopy, whereby the lineshape of the proton signal and the relaxation characteristics allow considerable insight into the motional and energetic properties of the water molecules that are closely associated with the macromolecules[12-14]. Child[15], for example, studied the n.m.r. proton relaxation of hydrated celluloses over the temperature range from 223 to 323 K. A slight increase in the transverse relaxation above 290 K was observed, which was (qualitatively) attributed to the existence of a small percentage of high-binding-energy water sorption sites, which are assumed to be found in the crystalline region of the cellulose. A sharp increase in the $T_2$ values was observed in the 5 to 10 wt% water regain, which is also the maximum bound water content in cellulose. Similar results have been obtained by Froix and Nelson[16] for hydrated cotton linters. Hale[17] recently studied various cellulose–water systems by pulsed n.m.r. spectroscopy, where the relaxation data were explained by two possible models. The first model describes the water as being bound perpendicular to the H–H vector and rapidly

* To whom correspondence should be addressed

0032-3861/94/13/2749-10

reorienting about this axis. The second possibility is that a small fraction of hydrogen-bound water exists, which slowly rotates about the O–H bond. By analysing the proton signal lineshape, Fleming *et al.*[18] were able to show that tightly bound water yields a doublet signal due to its preferential orientation. At higher temperatures, however, a singlet appears which was attributed to a more mobile, less tightly bound water phase. From lineshape analyses of the proton signal of hydrated celluloses Forslind[19] found that the *very tightly bound* water does not contribute to the water signal and it was therefore labelled *invisible* water.

The objective of this study was to investigate the possibility of identifying the different types of water based on their n.m.r. relaxation *versus* temperature characteristics. Motional properties modulate the nuclear magnetic relaxation of nuclei, which is the basis of the Bloembergen, Purcell, and Pound (BPP) theory[20]. Modified by Woessner[21] and Resing[22], this theory is capable of simulating the temperature dependence of the proton relaxation of anisotropically moving waters in heterogeneous materials. The environment in such systems usually provides the water with different types of sorption sites, each with its own individual distribution of binding energies. Such water tends to have a preferential orientation which leads to anisotropic reorientations. Therefore, motional anisotropy and energetic heterogeneity must be taken into account when interpreting the relaxation data of sorbed water molecules.

## EXPERIMENTAL

### *Sample preparation*

Sodium carboxymethylcellulose (NaCMC) powder (80 mesh) with a degree of substitution of 0.6 was purchased from Wako Pure Chemicals and used as received. A 5% (wt/vol) solution was prepared by adding the NaCMC powder slowly to deionized water and stirring for 24 h to ensure homogeneity. The viscous solution was transparent and no undissolved material was observed visually. The solution was divided into separate batches from which samples with water contents, $W_c$, ranging from 0.4 to 2.0 g g$^{-1}$ were prepared by partial evaporation. The $W_c$ of the studied samples is defined as

$$W_c = \frac{W_{H_2O}}{W_{dryCMC}} \quad (1)$$

where $W_{H_2O}$ and $W_{dryCMC}$ are the weights of the sorbed water and the dry carboxymethylcellulose, respectively. Samples were put in sealed sample containers and allowed to equilibrate for 24 h at room temperature, after which they were stored at −4°C until use. The appearance of the specimens ranged from a coarse powder ($W_c = 0.44$ g g$^{-1}$) to an elastic, gel-like substance ($W_c = 2.05$ g g$^{-1}$). For the n.m.r. experiments the conditioned samples were sealed in n.m.r. glass capillary tubes. The vials fitted snugly into the probe coil of the magnet. The full sample tubes were weighed before and after the experiments, and it was found that no weight loss occurred during the measurements.

### *N.m.r. measurements*

Proton spin–lattice ($T_1$) and spin–spin ($T_2$) relaxation times and broad-line lineshapes of the proton signals were recorded at a resonance frequency of 300.13 MHz with a Bruker 300MSL n.m.r. spectrometer connected to a wide bore superconducting electromagnet. Data collection was carried out at temperatures ranging from 330 to 120 K. Starting at 330 K, the experiments were performed in general at temperature intervals of 10 degrees. At the temperature region, $\Theta_{min}$, where the $T_1$ values pass through a minimum ($T_{1\,min}$), the step size was reduced to 5 degrees. The lineshapes were recorded by applying a 90° pulse with quadrature detection. The delay time was $5 \times T_1$. The sweep width was varied from 125 kHz in the motional narrowing region to 1 MHz at $T < 200$ K. Except for temperatures below 150 K, four repetitions were averaged. The $T_1$ values were measured with the inversion recovery method, and the $T_2$ values by applying the spin-echo method (the Gill–Meiboom variant of the Carr–Purcell method). At temperatures below 170 K, the solid-echo method was used. The temperature was controlled by a Bruker temperature controller which kept the sample temperature stable at ±1 K. Measurements were started at 330 K, with each cooling step (~3 K min$^{-1}$) followed by a 20 min equilibration step before the experiments commenced.

## RESULTS AND DISCUSSION

The following discussion is based on the relaxation and lineshape data which were recorded for hydrated sodium carboxymethylcellulose (NaCMC) samples having three different water contents, namely 0.44, 0.91, and 2.05 g g$^{-1}$. Up to a water content of 0.9–1.0 g g$^{-1}$ hydrated NaCMC does not show a freezing transition when it is slowly cooled from room temperature[1,23]. This implies that the two samples where $W_c = 0.44$ and 0.91 g g$^{-1}$ contain only non-freezing water, while in the sample with $W_c = 2.05$ g g$^{-1}$ freezing water makes up 50 wt% of the sorbed water.

### *Proton relaxation*

For all three samples the proton inversion recovery intensities are exponential, and only one $T_1$ component is observable over the entire temperature range. On the other hand, the spin-echo signals show a two-parameter exponential decay for temperatures above 160–180 K, below which only one $T_2$ component is observed. The short $T_2$s do not vary with temperature, are scattered around 50 μs, and are caused by the hydroxyl protons of the substrate. These observations are consistent with other relaxation results derived from sorbed water on silica gel[21] and cellulose[16].

The temperature dependence of the $T_1$ and $T_2$ values for the samples with water contents of 0.44, 0.91, and 2.05 g g$^{-1}$ is illustrated in *Figure 1*. Dashed lines represent $T_1$ and $T_2$ of an ideal ensemble of freely and isotropically tumbling protons of bulk water. These $T_1$ and $T_2$ values were calculated by applying the BPP theory without the consideration of distributed correlation times[20]. Several features distinguish the relaxation data of the hydrated NaCMC samples from the calculated $T_1$ and $T_2$ curves. First, the ratio of $T_1/T_2$ is far higher than the theoretical value of 1.6 at $\Theta_{min}$. This fact indicates that the proton correlation times of the above samples are distributed. Secondly, unlike the theoretical $T_1$ and $T_2$ curves, the measured values of $T_1$ and $T_2$ do not become equal at temperatures higher than $\Theta_{min}$. Instead, above 250 K, the $T_2$ values increase with decreasing temperatures. Similar observations have been reported for water on charcoal[24],

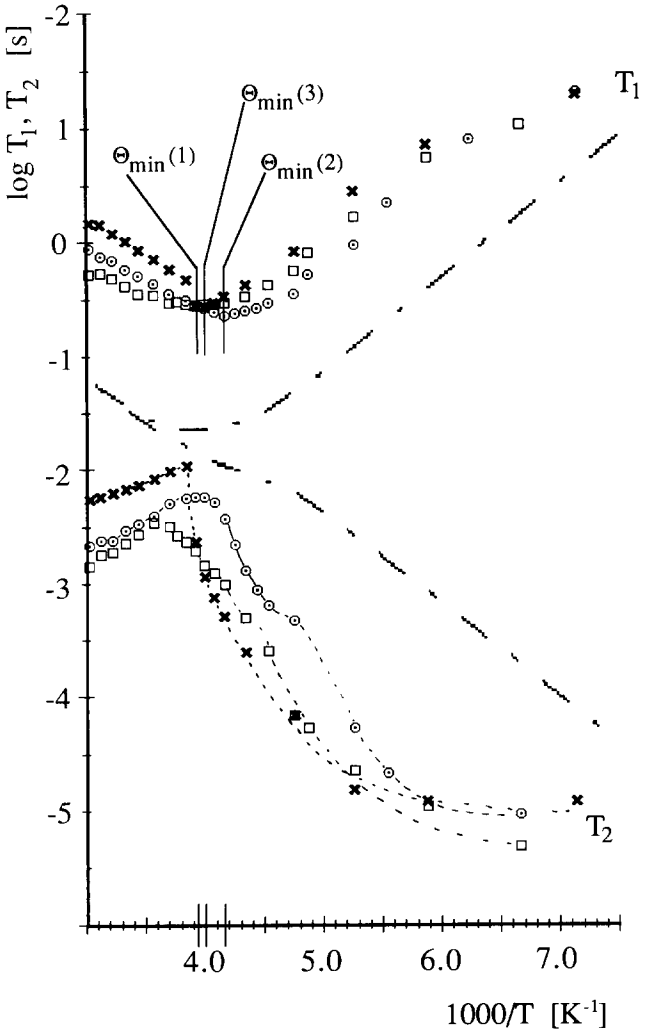


**Figure 1** Longitudinal (top) and transverse (bottom) relaxation times, $T_1$ and $T_2$, respectively, of samples of the water–NaCMC system with different water contents, as a function of inverse temperature: (□) 0.44 g $g^{-1}$; (⊙) 0.91 g $g^{-1}$; (×) 2.05 g $g^{-1}$; $\Theta_{min}(1)$ $T_{1\,min}$, $W_c = 0.44$ g $g^{-1}$; $\Theta_{min}(2)$ $T_{1\,min}$, $W_c = 0.91$ g $g^{-1}$; $\Theta_{min}(3)$ $T_{1\,min}$, $W_c = 2.05$ g $g^{-1}$: (– · –) theoretical $T_1$ and $T_2$ curves, calculated for freely tumbling water molecules using the BPP theory; single correlation time, no rigid lattice correction, $\sigma_0^2 = 1.57 \times 10^{10}$ $s^{-2}$ and $E_a = 16$ kJ $mol^{-1}$

silica gel[21], and to a lesser extent, on hydrated cellulose[15]. This phenomenon is usually explained by a two-phase distribution of sorption barrier heights, where a small amount of high-energy sites can dominate the measured $T_2$ at high temperatures[14]. Thirdly, the $T_2$s of the two samples with $W_c = 0.44$ and 0.91 g $g^{-1}$ do not decrease continuously with temperature, but exhibit a two-step decline. This is a manifestation of the anisotropic motional character of the sorbed water molecules where the correlation times of the rotational and the diffusional components have different activation energies and jump frequencies. This phenomenon is not observed for the sample where $W_c = 2.05$ g $g^{-1}$. The fourth feature observed is that at temperatures below 210 K, the $T_2$ value levels off at $\sim 10^{-5}$ s, which is equal to the $T_2$ of the immobilized rigid lattice protons, $T_{2\,rig}$.

Taking the above described anomalies into account an attempt was made to fit a modified BPP theory[21,22] to the experimental relaxation data by the numerical integration of

$$T_1^{-1} = \tfrac{2}{3}\sigma_0^2 \int_0^\infty P(\tau)\left(\frac{\tau}{1+\omega^2\tau^2} + \frac{\tau}{1+4\omega^2\tau^2}\right) d\tau \quad (2)$$

and

$$T_2^{-1} = \sigma_0^2 \int_0^\infty P(\tau)\left(\tau + \frac{5}{3}\frac{\tau}{(1+\omega^2\tau^2)} + \frac{2}{3}\frac{\tau}{(1+4\omega^2\tau^2)}\right) d\tau \quad (3)$$

where $P(\tau)$ is the distribution of correlation times $\tau$, and $\omega$ is the spectrometer frequency; $\sigma_0^2$ is the Van Vleck second moment of the resonating protons. Several types of $P(\tau)$ have been proposed. Among these a log-normal distribution seems to be the most adequate for the study of hydrated systems[14,22]. Described in detail by Nowick and Berry[25], the log-normal distribution can be written as

$$P(\tau)\,d\tau = \frac{\exp(z^2/\beta_{LN}^2)}{\sqrt{\pi}\beta_{LN}}\,dz \quad (4)$$

where $\beta_{LN}$ is the spread parameter of the log-normal distribution and $z = \ln(\tau/\tau^*)$, with $\tau^*$ as the most probable value of $\tau$. The correlation time at $\Theta_{min}$ can be fixed since the relationship $\omega\tau = 0.6158$ holds also if a distribution of correlation times with a constant $\beta_{LN}$ is applied. From this value of $\tau$ the correlation times as a function of temperature were calculated by applying an Arrhenius-type thermal activation law with the activation energy, $E_a$, as an adjustable parameter, where $E_a$ is a measure of the energy barrier heights at the water sorption sites. Additionally, a correction as described by Resing[22] has been applied to equation (3) to account for the temperature fraction of the rigid lattice protons which do not contribute to the spin–spin relaxation. The cut-off correlation time, $\tau_c$, is a function of the second moment $\sigma_0^2$ and is equal to the low temperature rigid lattice $T_{2\,rig}$ plateau value. This means that protons which reorient with frequencies of less than $\sim 10^5$ Hz were not included in the calculation of $T_2$. The second moment of the water protons is a structural parameter, depending on proton configurations, and is independent of temperature. It can be determined either from the rigid lattice value of the transverse relaxation, $T_{2\,rig}$, according to

$$T_{2\,rig} = \sqrt{\frac{\pi}{2\sigma^2}} \quad (5)$$

or from a comparison of the experimental value of $T_{1\,min}$ at $\Theta_{min}$ with the one calculated from equation (2) after choosing an appropriate spread parameter $\beta_{LN}$. From theoretical calculations based on possible proton arrangements[14], $\sigma_0^2$ must be between $1.57 \times 10^{10}$ and $2.63 \times 10^{10}$ $s^{-2}$. Although the values of the second moment as derived from equation (5) and from the calculation of $T_{1\,min}$ should both be theoretically the same, it was found that they differ by a factor of about 20. Applying a log-normal distribution of correlation times with $\beta_{LN} = 3.5$, the second moment which is calculated in accordance with equation (5) is $2.35 \times 10^{10}$ $s^{-2}$. This value was also used to fit equation (3) to the experimental $T_2$ data of all of the three samples with different water contents. This value is within the theoretically acceptable range for water dipolar relaxation. On the other hand, the second moment which is necessary to fit equation (2) to the experimentally determined values of $T_1$ is $1.22 \times 10^9$ $s^{-2}$, which is well below the second moment

of any possible water configuration. As shown in *Figure 2* (solid line connecting the $T_1$ data points), the BPP simulation of the $T_1$ data sets of all three samples can only be carried out with the application of single correlation times. This calls into question the underlying assumption of the BPP theory that both of the relaxation times, $T_1$ and $T_2$, are caused by the same motional characteristics of the water protons. However, $T_1$ is also a function of proton exchange between the hydroxyl group of the sorption site and the sorbed water molecules and a similar low second moment has been found for hydrated cellulose by Hsi *et al.*[26]. By taking site-water exchange relaxation and an increase of the average proton–proton distance, $r_{ij}$, into account a reduction of the second moment is expected. For example, only a small increase of the average $r_{ij}$ by 64% would result in a reduction of the second moment by a factor of 20, due to the dependence of the second moment on $r_{ij}^{-6}$ [26].

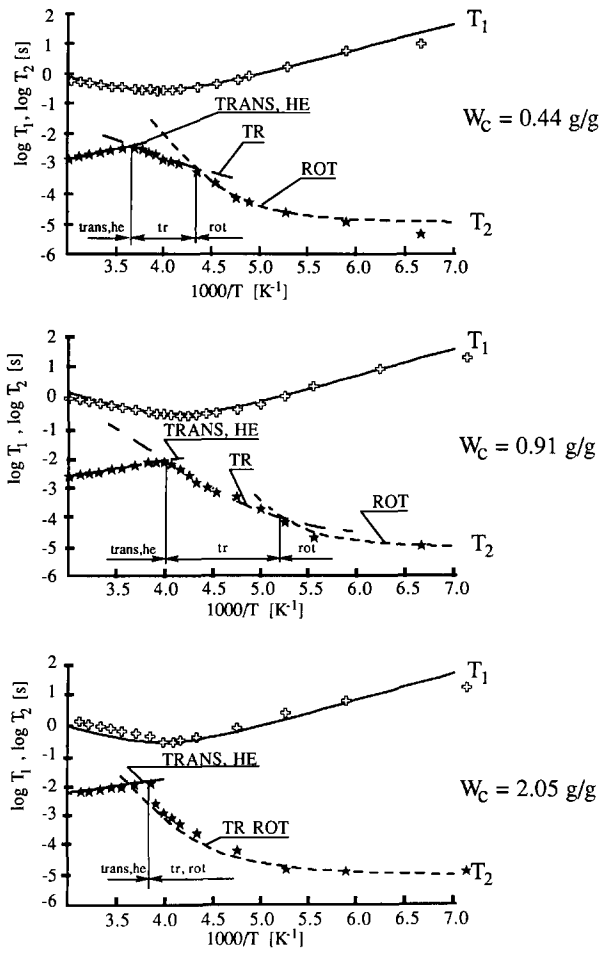


**Figure 2** Relationship between the experimental values of the longitudinal ($T_1$) and transverse ($T_2$) relaxation times of samples of the water–NaCMC system with different water contents, and the BPP simulations of the respective data (see also *Table 1*). (+) $T_1$, no distribution of correlation times. (★) $T_2$: trans, he high-energy site domination of $T_2$ (transition region); TRANS, HE calculated from equation (6) with no distribution of correlation times applied; tr frequency of translational motion of water molecules is higher than that of rotational motion; TR calculated from equation (3), activation energy ($E_a$(tr)) is function of water content, log-normal distribution of correlation times and rigid lattice correction applied; rot frequency of rotational motion of water molecules is higher than that of translational motion; ROT calculated from equation (3), activation energy ($E_a$(rot)) is independent of water content, log-normal distribution of correlation times and rigid lattice correction applied

*Binding energy heterogeneity*

Although the simultaneous fitting of both sets of relaxation data was not possible, the modelling of the $T_2$s as a function of temperature allows us to draw some conclusions about the motional state of the adsorbed water molecules. In all three samples the transverse relaxation passes through a maximum which ranges from 250 K ($W_c = 0.91$ and $2.05\,g\,g^{-1}$) to 280 K ($W_c = 0.44\,g\,g^{-1}$). At temperatures higher than these values, the $T_2$s decrease with increasing temperature. Resing[14] explained this anomaly by assuming that two or more fractions of water binding sites, with distinct different distributions of binding energies, exist. This would theoretically lead to a series of sequential $T_2$ *versus* temperature curves, each with its own rigid lattice plateau. Considering the case of two distinct sites, i.e. a high- and a low-energy site, a transition range can be observed where the apparent $T_2$ begins to increase with falling temperatures because of the reduced probability that a water molecule can jump out of the high energy well. In the experimental temperature range of this study, the above increase in the $T_2$ values was observed in the temperature range between 320 and 280 K ($W_c = 0.44\,g\,g^{-1}$), 320 and 250 K ($W_c = 0.91\,g\,g^{-1}$), and 320 and 260 K ($W_c = 2.05\,g\,g^{-1}$). Assuming a single high-energy correlation time, the slope of the transitional relaxation time, $T_2$(trans,he) is proportional to the high-energy correlation time, $\tau_{he}$ as follows:

$$T_2(\text{trans,he}) = \tau_{he}\frac{P_{he}}{P_{low}} \qquad (6)$$

where $P_{he}/P_{low}$ is the ratio of high-energy to low-energy sites[14].

At the temperature where $T_2$(trans,he) intersects with the relaxation-time line of the lower binding energy site protons, the apparent $T_2$ passes through a maximum, and below this temperature becomes equal to the $T_2$ values of the protons that are bound with lower binding energies. If the distribution function of $\tau$ were known exactly, it would be possible to calculate the relative abundance and the average binding energies for the high-energy sites from the $T_2$(trans,he) data. However, it was impossible to unambiguously choose a distribution function because of the limited temperature range over which the transitional $T_2$(trans,he) values were measured. It was therefore not feasible to quantify the percentage of water molecules bound at the high-energy sites or to estimate their average binding energies. The lines drawn through the $T_2$(trans,he) data in *Figure 2* were calculated assuming no distribution of correlation times, i.e. binding energies. However, it is possible to examine the relative changes of the fraction of higher energy binding sites with the changing water contents. The slope, shape and position of the experimental transition curve is seemingly a function of water content where the curves become somewhat flatter and the absolute values increase with higher water contents. Flattening of the curve qualitatively means that either the average values of the binding energies are reduced or their distribution becomes wider. Assuming that the distribution of binding energies is constant and is not a function of water content, the apparent reduction of the activation energy indicates that the ease by which the water molecules can jump out of the high-energy well increases with water content. Furthermore, the increase of the $T_2$(trans,he) transition temperatures with increasing water content is the result

of an increase in the ratio of low-energy to high-energy sites, $P_{he}/P_{low}$. However, no conclusive statement can be made about the absolute number of high-energy sites and whether their number is a function of total water content, although there is a possibility that the number of high-energy sites is constant. It has been suggested that in cellulose these sites can be found in the crystalline region of the substrate[15]. In the system under investigation here, however, no crystalline morphology exists. Nevertheless, water is not only associated with the host molecule, but also forms a shell of hydration around the counterions. The presence of counterions contributes significantly to the maximum amount of non-freezing water, and it has been found that the amount of the latter which is associated with the ion is a function of its radius[6]. With respect to the observations described above, it is possible that the ion binding sites and the high-energy binding sites are identical.

*Motional anisotropy*

The other important feature of the relaxation data is the apparent two-step decline of the $T_2$ values in the two samples with $W_c = 0.44$ and $0.91\ g\ g^{-1}$. This is most likely the result of the anisotropic nature of the molecular motion of the sorbed water molecules. Water molecules, even if they are non-freezing, undergo rotational and translational motions whereby the latter also leads to diffusion of the molecules throughout the solid[8,14]. The rotational and translational components of the molecular motion may be distinguished by their frequency and activation energies. The correlation times of both components, $\tau_{rot}$ and $\tau_{tr}$ are a function of temperature, but in bulk water, $\tau_{rot} = \tau_{tr}$ and the two components cannot be distinguished by relaxation analysis. By partitioning the second moment into a translational and rotational component, $k_{rot}\sigma_0^2$ and $k_{tr}\sigma_0^2$, respectively, where $k_{rot} + k_{tr} = 1$, equation (3) can be modified to adequately fit the stepwise decline of $T_2$ (see *Figure 2*, lines ROT, TR, and *Table 1*).

At moderately high temperatures the $T_2$ values are dominated by translational motion while at lower temperatures the rotational correlation times become shorter and the experimental values are caused by molecular rotation. This can be observed for the low-water-content samples ($W_c < 1.0\ g\ g^{-1}$) which do not contain freezing water. Such a separation of jump frequencies was demonstrated for benzene adsorbed on to silica[27] and charcoal[28]. On the other hand, it was not possible to separate the $T_2$ data of the sample with $W_c = 2.05\ g\ g^{-1}$ by the modified BBP simulation and it was therefore assumed that the rotational and diffusional correlation times are equal ($\tau_{rot} = \tau_{tr}$). The above result agrees with the n.m.r. studies of bulk water[20] and other hydrated organic systems[21,24] where it is usually found that $\tau_{rot} = \tau_{tr}$ and no separation of the transverse relaxation is possible. The rotational activation energies of the molecular motion, $E_a$(rot), are 75 kJ mol$^{-1}$ and are independent of water content. $E_a$(tr), however, increases with water content and eventually, at $W_c = 2.05\ g\ g^{-1}$, also becomes 75 kJ mol$^{-1}$ (see *Table 1*). This implies that the frequency of rotational jumps is independent of water content while translational mobility increases with an increased presence of sorbed water. This phenomenon is also responsible for the decrease of the temperature, where $\tau_{rot} = \tau_{tr}$, with increasing water content. Thus, the increased presence of water facilitates the translational and diffusional movements of sorbed water molecules while the rotational component is not affected.

*Lineshape analysis*

At temperatures below 200 K the rotational frequency of the water molecules falls below the rigid lattice threshold. In this temperature range, relaxation analysis by itself is not capable of addressing the influence of water content on water mobility. Therefore, in this low-temperature range, in addition to relaxation analysis, the recording of the signal lineshape yields supplementary information. From the recorded proton n.m.r. lineshapes of the NaCMC samples (*Figure 3*) it can be seen that above a temperature of about 210 K line broadening is minimal. Although samples with water content of $2.05\ g\ g^{-1}$ contain freezing water which forms ice below 250 K, this transition did not influence the lineshape. At ~200 K line broadening commences and at 150 K the lineshape changes to a broadened doublet with a superimposed central singlet. The peak-to-peak separation of the low-temperature signals of the hydrated NaCMC samples is of the order of $5 \times 10^{-4}$ T which suggests that the doublets are caused by immobilized rigid lattice proton pairs. According to the Pake theory[29], stationary proton pairs will give rise to a doublet signal, $p(\Delta H)$, where the shoulder-to-shoulder distance is a

**Table 1** Parameters used to fit the BPP theory (equations (2) and (3)) to the spin–lattice ($T_1$) and spin–spin ($T_2$) relaxation data of the water–NaCMC systems

| Water content ($g\ g^{-1}$) | $\theta_{min}$[a] (K) | Activation energy, $E_a$ (kJ mol$^{-1}$) | | | | Second moment, $\sigma_0^2$ ($10^{10}\ s^{-2}$) | | | | Spread parameter $\beta$ (log-normal distribution of $\tau$) | |
|---|---|---|---|---|---|---|---|---|---|---|---|
| | | $T_1$ | $T_2$ | | | $T_1$ | $T_2$ | | | | |
| | | | HE[b,e] | TR[c] | ROT[d] | | Total | TR[c,f] | ROT[d,f] | $T_1$ | $T_2$ |
| 0.44 | 255 | 16 | 13 | 25 | 75 | 1.22 | 2.35 | 0.57 | 0.43 | 0 | 3.5 |
| 0.91 | 240 | 17 | 10 | 45 | 75 | 1.22 | 2.35 | 0.30 | 0.70 | 0 | 3.5 |
| 2.05 | 250 | 17 | 9 | 75 | 75 | 1.1 | 2.35 | – | – | 0 | 3.5 |

[a] Temperature of $T_{1\,min}$
[b] High-energy sites
[c] Translational motion component
[d] Rotational motion component
[e] Absolute values are not correct since no distribution of correlation times was applied
[f] Fraction of total second moment

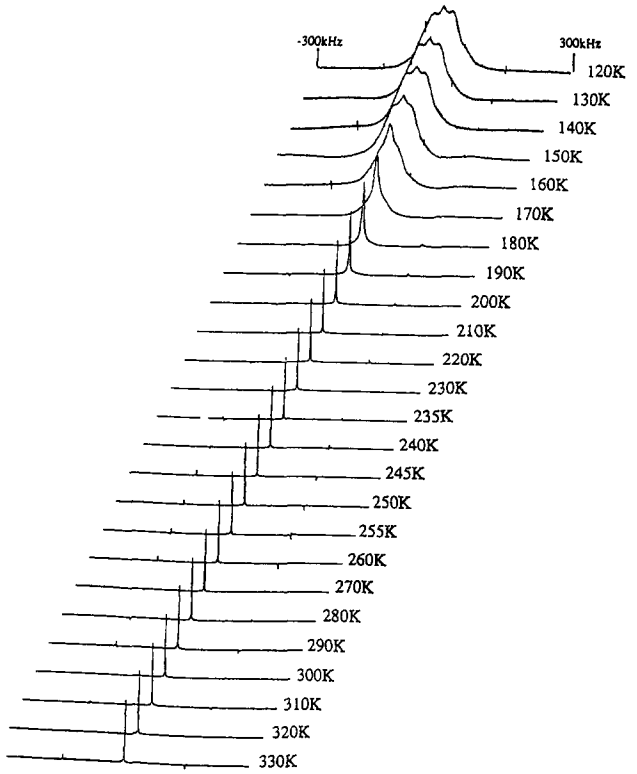


**Figure 3** Proton n.m.r. wide-line spectra of an aqueous NaCMC sample ($W_c = 0.91\ g_{H_2O}/g_{CMC}$) as a function of temperature

function of the inverse third power of the inter-proton distance, $r_{ij}$, such that

$$p(\Delta H) = \left(\frac{\Delta H}{\alpha} + 1\right)^{-1}_{[-\alpha \leqslant \Delta H \leqslant 2\alpha]} + \left(-\frac{\Delta H}{\alpha} + 1\right)^{-1}_{[-2\alpha \leqslant \Delta H \leqslant \alpha]} \quad (7)$$

where $\Delta H = H_0 - H^*$, $H_0$ is the resonance field, and $H^*$ is the local field; $\alpha = 3/4\mu r_{ij}^{-3}$ where $\mu$ is the nuclear magneton ($5.0505 \times 10^{-27}\ J\ T^{-1}$). Due to the individual line broadening of the randomly oriented proton pairs, the doublet is smoothened. This can be modelled by applying a line-broadening function $L(\Delta H)$ such that $P(\Delta H)$, the smoothened Pake function is

$$P(\Delta H) = \int_{-\infty}^{\infty} p(\Delta H) L(\Delta H)\, dH_0 \quad (8)$$

where $L(\Delta H)$ was chosen to be the Lorentzian function $1/\pi\ (\beta_L^2 + \Delta H^2)^{-1}$, with $\beta_L$ as the spread parameter.

Applying the Pake theory it was found that the inter-proton distance $r_{i,j}$ is $1.52 \pm 0.01$ Å. This clearly identifies the doublet as being caused by immobilized and isolated water molecules that do not contribute to the dipolar relaxation but are responsible for $T_{2\,rig}$. In the BPP calculation of $T_2$ the above water molecules were accounted for by virtue of the rigid-lattice cut-off correction[22]. The mobile water fraction at $T < 200$ K consists of slowly rotating non-diffusing molecules. Proton pairs which slowly rotate perpendicular to the H–H vector also cause a Pake doublet, but the shoulder-to-shoulder distance is half that of the rigid lattice doublet[30]. Because of their relative smaller widths, such 'rotating' Pake doublets often disappear due to individual line broadening and are not identifiable as doublets. For this reason, it is very likely that the central singlet of the low-temperature peaks is caused by rotating proton pairs. Nevertheless, it is analytically not possible to extract dimensional information from the recorded singlet lineshape, because it is unlikely that all of the water molecules rotate about the axis perpendicular to the inter-proton vector. Also, some relatively faster moving molecules may induce a narrowing effect. It was therefore decided to approximate the central peak with a simple Gaussian lineshape. With this in mind, the entire signal shape can be simulated as a composite curve which consists of a backbone (CMC) signal, a stationary water (Pake) signal, and a mobile (i.e. a rotating) water signal. Therefore, it is possible to calculate the relative abundance of the two types of water molecules as a function of temperature (*Table 2*).

Composite lineshapes consisting of (1) the Pake signal (stationary protons; equations (7) and (8); adjustable parameters, $r_{ij}$, $\beta_L$), (2) a Gaussian line (CMC backbone; adjustable parameter, $\beta_G$), and (3) another Gaussian line for the central signal (rotating water; adjustable parameter, $\beta_G$) were calculated to match the experimental curves. For the values of the adjustable parameters see *Table 2*. As representative examples, the simulated signal separations of the n.m.r. peaks recorded at 140 K for water contents of 0.91 and $2.05\ g\ g^{-1}$ are shown in *Figure 4*. The line-fitting results for all low temperature peaks of the samples with $W_c = 0.44\ g\ g^{-1}$ are shown in *Figure 5*. As can be seen, these calculated composite lineshapes very closely match the measured ones and as a result of this procedure it was possible to calculate the temperature dependence of the respective peak area fraction (i.e. the respective fraction of proton population, see *Table 2* and *Figure 6*). All three samples have a fairly stable amount of backbone proton population although in the case of the low-water samples they slightly decrease at higher temperatures. This may be attributed to the increasing uncertainty of identifying the backbone contribution above 170 K since its relative peak height decreases considerably when compared with the peak height of the narrowing water signals. Another explanation may be found be assuming that at very low temperatures ($T < 150$ K) a certain amount of water molecules is not sufficiently isolated from the backbone protons to cause a Pake-type response. Such waters would be equal to invisible water as it has been described by Forslind[19].

All three samples have in common the fact that even at temperatures below 150 K a small amount (1–2%) of the signal originates from mobile water. This level is constant up to a temperature of ~150–160 K, after which a sharp increase of the mobile water proton fraction and a decrease of the stationary proton fraction is observed (see *Figure 6*). This temperature has a general significance for hydrated water. For example, the slope of the molar heat capacity of hydrated macromolecules, as a function of temperature, changes distinctly at 150 K, which has been explained by the commencement of the cooperative motion of small, amorphous water aggregates[5]. At temperatures higher than 150 K the ratio of mobile (i.e. rotating) to immobile waters increase sharply, as long as the samples do not contain freezing water ($W_c < 1.0\ g\ g^{-1}$). The total water content in such systems does not seem to influence the respective ratios (see *Figure 7*). However, in the sample where the water content slightly exceeds

**Table 2** Fractional signal areas of the proton n.m.r. lines and adjustable parameters ($\beta_G$, $\beta_L$) for hydrated NaCMC

| Temperature (K) | Water content ($g_{H_2O}/g_{CMC}$) | Signal component: Central singlet (mobile water) Relative signal area | $\beta_G$[a] (kHz) | Broad peak (CMC protons) Relative signal area | $\beta_G$[a] (kHz) | Pake peak (stationary water) Relative signal area | $\beta_L$[b] (G) | Proton–proton distance $r_{ij}$ (Å) |
|---|---|---|---|---|---|---|---|---|
| | 0.44 | 0.018 | 4.7 | 0.679 | 61.0 | 0.303 | 1.6 | 1.52 |
| 120 | 0.92 | 0.020 | 4.0 | 0.556 | 57.5 | 0.430 | 1.6 | 1.52 |
| | 2.05 | – | – | – | – | – | – | – |
| | 0.44 | – | – | – | – | – | – | – |
| 130 | 0.92 | 0.019 | 5.5 | 0.56 | 48.0 | 0.418 | 1.6 | 1.52 |
| | 2.05 | – | – | – | – | – | – | – |
| | 0.44 | 0.010 | 2.5 | 0.665 | 28.1 | 0.325 | 1.6 | 1.52 |
| 140 | 0.92 | 0.014 | 6.0 | 0.568 | 45.0 | 0.042 | 1.6 | 1.52 |
| | 2.05 | 0.025 | 5.2 | 0.365 | 45.0 | 0.611 | 2.4 | 1.51 |
| | 0.44 | 0.018 | 4.0 | 0.668 | 28.0 | 0.315 | 1.6 | 1.52 |
| 150 | 0.92 | 0.027 | 6.0 | 0.568 | 34.0 | 0.405 | 1.6 | 1.52 |
| | 2.05 | 0.039 | 6.4 | 0.332 | 35.0 | 0.629 | 2.4 | 1.53 |
| | 0.44 | 0.048 | 5.4 | 0.627 | 27.9 | 0.275 | 1.6 | 1.52 |
| 160 | 0.92 | 0.080 | 6.1 | 0.370 | 32.0 | 0.550 | 1.6 | 1.52 |
| | 2.05 | – | – | – | – | – | – | – |
| | 0.44 | 0.125 | 6.0 | 0.581 | 24.5 | 0.294 | 1.6 | 1.52 |
| 170 | 0.92 | 0.250 | 5.0 | 0.351 | 19.5 | 0.391 | 1.6 | 1.52 |
| | 2.05 | 0.088 | 7.0 | 0.429 | 37.5 | 0.484 | | 1.53 |
| | 0.44 | 0.221 | 4.3 | 0.482 | 19.5 | 0.298 | 1.6 | 1.52 |
| 180 | 0.92 | 0.517 | 3.0 | 0.320 | 14.0 | 0.163 | 1.6 | 1.52 |
| | 2.05 | 0.212 | 5.0 | 0.310 | 22.0 | 0.478 | 2.4 | 1.53 |
| | 0.44 | 0.300 | 3.2 | 0.497 | 17.4 | 0.202 | 1.6 | 1.52 |
| 190 | 0.92 | – | – | – | – | – | – | – |
| | 2.05 | 0.296 | 4.2 | 0.333 | 11.5 | 0.371 | 2.4 | 1.53 |

[a] Gaussian spread parameter
[b] Lorentzian spread parameter of individual lines (random orientation of proton pairs); $IG = 10^{-4}T$

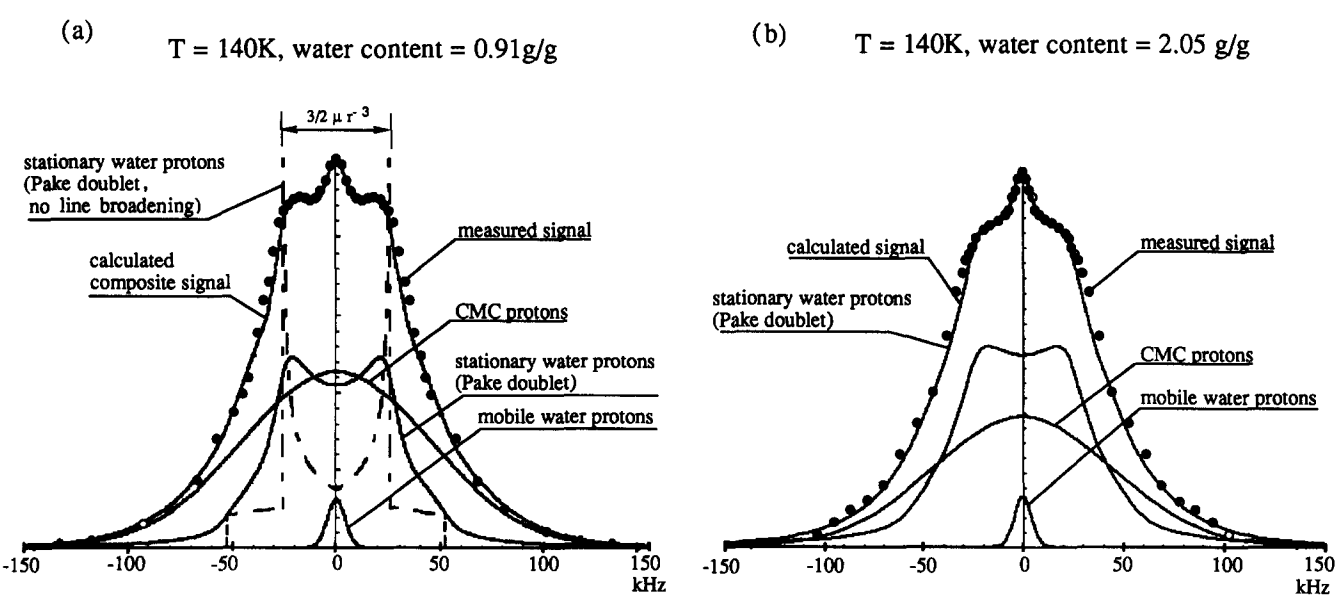


**Figure 4** Simulated peak separations of proton n.m.r. wide-line signals of aqueous NaCMC at 140 K (see also *Table 2*) with water contents, $W_c$, of (a) 0.91 $g_{H_2O}/g_{CMC}$, including non-line-broadened Pake signal (equation (7)) and (b) 2.05 $g_{H_2O}/g_{CMC}$: r = proton–proton distance; nuclear magneton, $\mu = 5.0505 \times 10^{-27}$ J $T^{-1}$

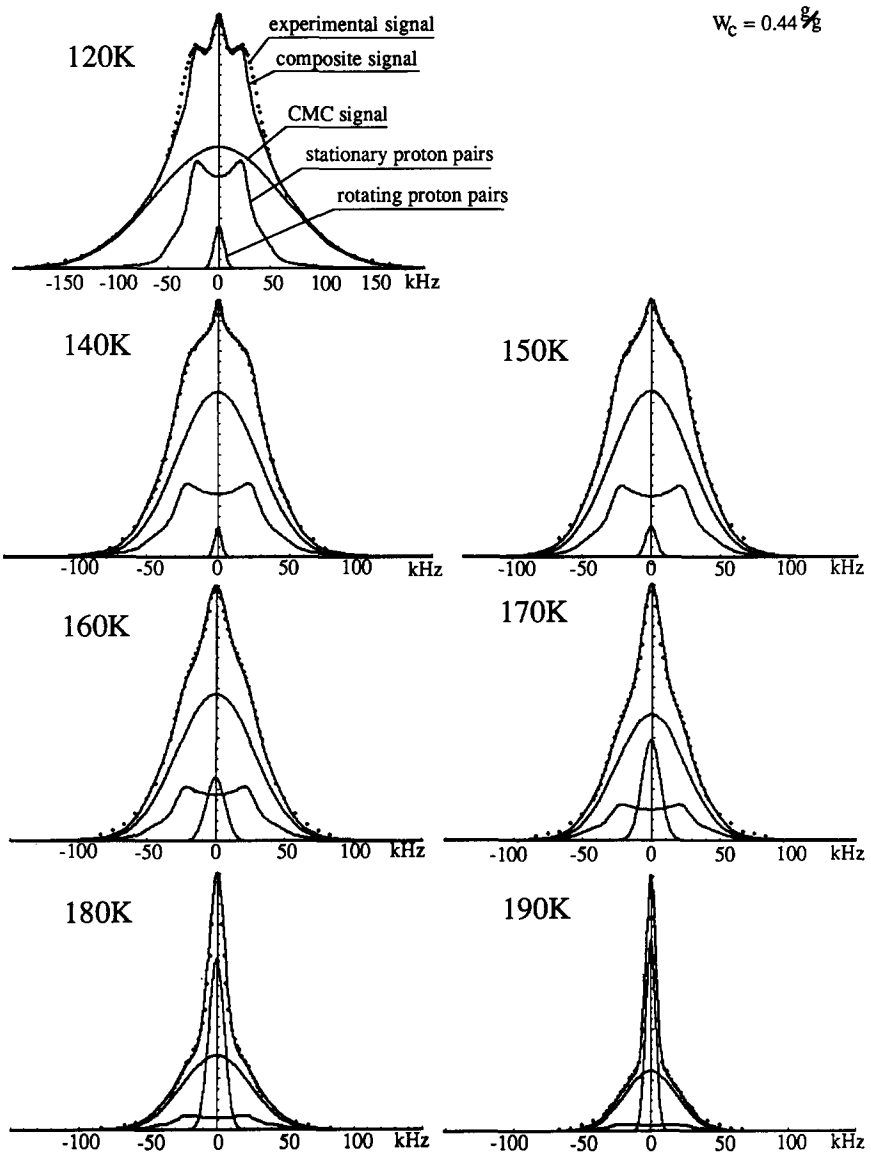


**Figure 5** Compilation of normalized, simulated and measured lineshapes of the water–NaCMC system at low temperatures (120–190 K); $W_c = 0.44$ $g_{H_2O}/g_{CMC}$

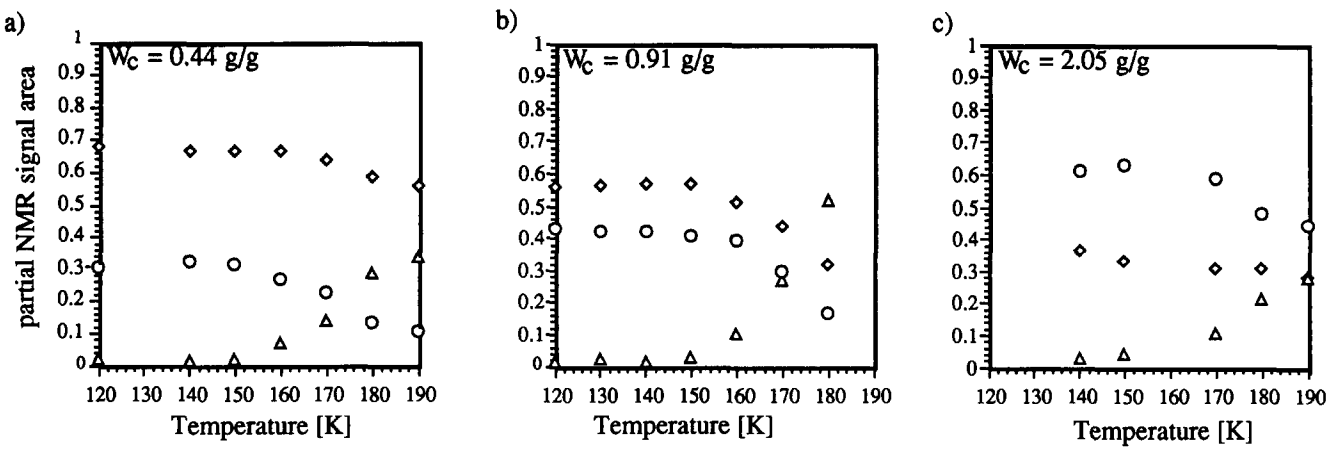


**Figure 6** Temperature dependence of the peak area fraction of the CMC (◇), rigid lattice (○), and mobile water (Δ) proton n.m.r. signals for aqueous NaCMC systems with water contents of: (a) 0.44 $g_{H_2O}/g_{CMC}$; (b) 0.91 $g_{H_2O}/g_{CMC}$; (c) 2.05 $g_{H_2O}/g_{CMC}$

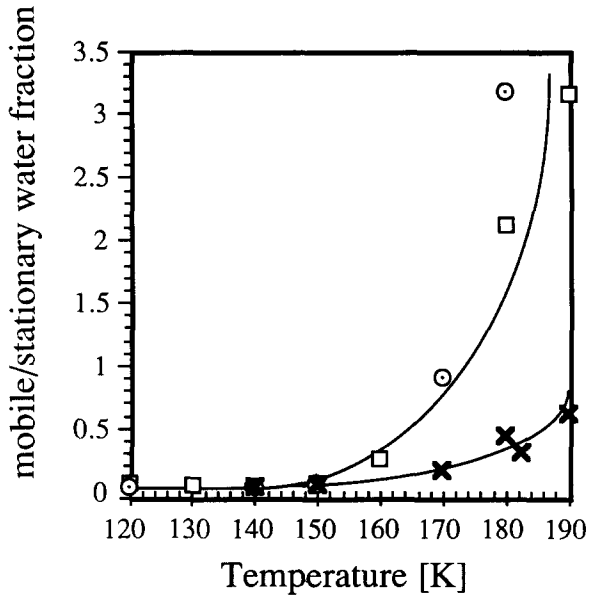


**Figure 7** Ratio of mobile to stationary water fraction as a function of temperature, as calculated from the respective area fractions of the backbone, rigid lattice, and mobile water proton n.m.r. signals of the aqueous NaCMC system: (□) 0.44 $g_{H_2O}/g_{CMC}$; (⊙) 0.91 $g_{H_2O}/g_{CMC}$; (×) 2.05 $g_{H_2O}/g_{CMC}$

the maximum non-freezing water content the relative concentration of mobile waters is considerably smaller. In this case, the presence of ice restricts the mobility of rotating, non-freezing water at temperatures below 200 K. The observation that the presence of ice restricts the mobility of non-freezing water agrees well with another study carried out on sodium cellulose sulfate[1]. At temperatures higher than 200–210 K the influence of the water content on the rotational component ceases, as shown by the above relaxation analysis.

## CONCLUSIONS

In aqueous sodium carboxymethylcellulose samples with water contents of less than 2.05 g $g^{-1}$, at least two classes of non-freezing water can be identified by the dipolar relaxation characteristics of their protons. The first category of non-freezing water consists of water molecules which are associated with sites where the binding energy is substantially higher than at other sites. The proton pairs of these water molecules dominate the spin–spin relaxation at temperatures above 250 K. Below this temperature, $T_2$ is controlled by water being attached to low-energy sites, most likely on the CMC backbone. These molecules show motional anisotropy with a rotational and translational component. If freezing water is not present (i.e. $W_c < 1$ g $g^{-1}$), both components have different correlation times ($\tau_{rot}$, $\tau_{tr}$). At $T > 200$ K, $\tau_{rot}$ is independent of water content, while $\tau_{tr}$ increases with water content. Below the cross-over temperature where $\tau_{min} = \tau_{tr}$, the rotational frequency of the water molecules is higher than the translational frequency. The temperature where the spin–spin relaxation changes from a translational jump to a rotational modulation decreases with water content. Therefore, translational jumps are facilitated by the presence of extra water but the rotational component is not affected. If the system contains freezing water (i.e. $W_c > 1$ g $g^{-1}$), $\tau_{rot}$ becomes equal to $\tau_{tr}$ at all temperatures, which is not unlike the situation found in free water. At temperatures below 200 K the movement of an increasing fraction of the rotating sorbed water molecules becomes too slow to affect the relaxation data that cause the line broadening of the n.m.r. signal. At these temperatures the signal has a composite lineshape, and includes the Pake doublet, which is typical of stationary, non-rotating proton pairs. Their relative abundance increases steadily with decreasing temperature while the fraction of rotating molecules reduces. The ratio of stationary to mobile water is the same for samples which contain only non-freezing water. Thus, water content does not influence the mobility at temperatures below 200 K, as long as the samples do not contain freezing water. The presence of freezing water in the form of ice considerably reduces the fraction of mobile (i.e. rotating) water molecules at these temperatures. At 150 K, the amount of immobilized water molecules reaches a constant maximum value, where almost all motion of the sorbed water ceases. However, even at temperatures as low as 120 K, 1–2% of mobile protons remain sufficiently mobile to cause a narrow signal line component.

## ACKNOWLEDGEMENTS

The authors wish to express their gratitude to Dr Tatsuko Hatakeyama for her valuable contributions to the discussions of this work and to Dr Yukiyo Hiroyama of Bruker Instruments for her help in setting up the relaxation experiments.

## REFERENCES

1 Hatakeyama, H. and Hatakeyama, T. in 'Properties of Ionic Polymers – Natural and Synthetic', (Eds L. Salmén and M. Htun), Swedish Pulp and Paper Institute, Stockholm, 1991, 123
2 Berendsen, H. J. C. in 'Water, A Comprehensive Treatise' (Ed. F. Franks), Vol. 5, Plenum Press, New York, 1975, Ch. 6, p. 293
3 Sugget, A. in 'Water, A Comprehensive Treatise' (Ed. F. Franks), Vol. 4, Plenum Press, New York, 1975, Ch. 6, p. 519
4 Rowland, S. P. and Kuntz Jr, I. D. in 'Water in Polymers' (Ed. S. S. Rowland), ACS Symp. Ser. No. 127, American Chemical Society, Washington DC, 1980, p. 1
5 Hoeve, G. A. in 'Water in Polymers' (Ed. S. S. Rowland), ACS Symp. Ser. No. 127, American Chemical Society, Washington DC, 1980, p. 135
6 Nakamura, K., Hatakeyama, T. and Hatakeyama, H. *Textile Res. J.* 1981, **51**, 607
7 Hatakeyama, T., Hatakeyama, H. and Nakamura, K. *Thermochim. Acta* 1988, **123**, 153
8 Kinard, D. A. and Hoeve, C. A. J. *J. Polym. Sci. Polym. Symp. Edn* 1984, **71**, 183
9 Nakamura, K., Hatakeyama, T. and Hatakeyama, H. in 'Wood and Cellulosics: Industrial Utilization, Biotechnology, Structure, and Properties' (Eds J. F. Kennedy, G. O. Phillips and P. A. Williams), Ellis Horwood, Chichester, 1987, p. 97
10 Hatakeyama, H. and Hatakeyama, T. in 'Cellulose: Structural and Functional Aspects' (Eds J. F. Kennedy, G. O. Phillips and P. A. Williams), Ellis Horwood, Chichester, 1989, 131
11 Deodhar, S. and Luner, P. in 'Water in Polymers' (Ed. S. S. Rowland), ACS Symp. Ser. No. 127, American Chemical Society, Washington DC, 1980, p. 273
12 Pfeifer, H. in 'NMR, Basic Principles and Progress' (Eds P. Diel, E. Fluck and R. Kosfeld), Vol. 7, Springer, Berlin, 1972, p. 53
13 Pfeifer, H. *Phys. Rep.* 1976, **26**, 293
14 Resing, H. A. *Adv. Mol. Relaxation Processes* 1967, **1**, 109
15 Child, T. F. *Polymer* 1972, **13**, 259
16 Froix, M. F. and Nelson, R. *Macromolecules* 1975, **8**, 726
17 Hale, M. E. *Diss. Abstr. Int.* 1991, **5**, 5389-B

18 Flemming, W. W., Fornes, R. E. and Memory, J. D. *J. Polym. Sci. Polym. Phys. Edn* 1979, **7**, 199
19 Forslind, E. in 'NMR Basic Principles and Progress' (Eds P. Diel, E. Fluck and R. Kosfeld), Vol. 4, Springer, Berlin, 1971, p. 145
20 Bloembergen, N., Purcell, E. M. and Pound, V. R. *Phys. Rev.* 1948, **73**, 679
21 Woessner, D. E. *J. Chem. Phys.* 1963, **39**, 2783
22 Resing, H. A. *J. Chem. Phys.* 1965, **43**, 669
23 Hofmann, K., Hatakeyama, H. and Hatakeyama, T. *Sen-I Gakkai Prepr.* 1992, 180
24 Resing, H. A., Thompson, J. K. and Krebs, J. J. *J. Phys. Chem.* 1964, **68**, 1621
25 Nowick, A. S. and Berry, B. S. *IBM J. Res. Devel.* 1961, **5**, 297
26 Hsi, E., Vogt, G. J. and Bryant, R. G. *J. Colloid Interface Sci.* 1979, **70**, 338
27 Woessner, D. E. and Zimmerman, J. R. *J. Phys. Chem.* 1963, **67**, 1590
28 Thompson, J. K., Krebs, J. J. and Resing, H. A. *J. Chem. Phys.* 1965, **43**, 3853
29 Pake, G. E. *J. Chem. Phys.* 1948, **16**, 327
30 Gutowsky, H. S. and Pake, G. E. *J. Chem. Phys.* 1950, **18**, 162